

SUPPLEMENTARY INFORMATION FOR

A VOLTAGE-SENSOR WATER PORE

J. Alfredo Freites¹, Douglas J. Tobias², and Stephen H. White^{3*}

¹Institute for Genomics and Bioinformatics, ²Department of Chemistry and Institute
for Surface and Interface Science, ³Department of Physiology and Biophysics,
University of California, Irvine, CA 92697, USA

*To whom correspondence should be addressed: University of California at Irvine,
Dept. of Physiology and Biophysics, Medical Sciences I - D346, Irvine, CA 92697-4560.
Phone: 949-824-7122. FAX: 949-824-8540. e-mail: stephen.white@uci.edu

Methods

Our VS atomistic model corresponds to KvAP residues 24 to 147 in the model proposed by MacKinnon and his collaborators for the full channel (1). This includes the TM segments S1-S4 and the S4-S5 connector. Extracting the VS from the whole channel model allows a simple, unequivocal, choice for the initial configuration of the system, as the location of the channel pore in the lipid bilayer is well defined.

Hydrogen atoms were added with psfgen, a stand-alone structure building tool part of the NAMD package (2), using the molecular topologies provided with the CHARMM force field (3). The initial structure was submitted to three rounds of 5000-step conjugate-gradient energy minimization, 50 ps of molecular dynamics at 600 K, and 100 ps of molecular dynamics at 300 K. During these runs, all hydrogen atoms were free to move, and all the non-hydrogen atoms were fixed.

The relaxed model of the VS domain was then inserted into a previously equilibrated all-atom POPC model bilayer with excess water. Initially, the insertion was performed by aligning the protein principal axis with the bilayer TM direction and placing the centers-of-mass of the bilayer system and the protein at the origin of coordinates. The final location was adjusted following the prescriptions indicated in Lee et al. (1) : the S4-S5 linker, the tyrosines in the S1-S2 connector, and the S3b-S4 loop should be located at the bilayer interfaces. The lipid molecules from each bilayer leaflet that overlapped with the protein chain were removed from the system. The final system was composed of the VS domain (124 aminoacid residues), 232 lipid molecules, 12109 water molecules, and 2 negative counter-ions, for a total of 69430 atoms. The dimensions of the initial simulation cell were $88.9070 \times 90.4187 \times 86.5884$ Å.

The initial system equilibration process consisted, first, of 10000 steps of energy minimization, followed by a 700 ps molecular dynamics run at constant volume and constant temperature (300 K) over the lipid molecules that formed the first coordination shell of the protein. This was followed by a run over all the lipid molecules, consisting of 5000 steps of energy minimization and 2 ns molecular dynamics run at constant volume and constant temperature (300 K). This rather long run was necessary to allow the lipids to line closely and uniformly the surfaces of the protein domain, thereby guarantying that no waters or counter-ions would penetrate the bilayers during the equilibration process. The final step of the initial equilibration

process was a run over lipids, waters, and counter-ions consisting of 5000 steps of energy minimization, followed by a 500 ps molecular dynamics run at constant volume and constant temperature (300 K). The full simulation was then carried out at constant temperature of 300 K and constant pressure of 1 atm. The protein was progressively released from its initial configuration over ten 200 ps steps, each using harmonic restraints.

All the molecular dynamics runs were conducted with the NAMD 2.5 software package (2). The CHARMM22 and CHARMM27 force fields (3, 4) were used for the peptide and the lipids, respectively, and the TIP3P model was used for water (5). The smooth particle mesh Ewald (PME) method (6, 7) was used to calculate electrostatic interactions, and the short-range real-space interactions were cut off at 11 Å, employing a switching function. A reversible multiple time-step algorithm (8) was employed to integrate the equations of motion with a time step of 4 fs for electrostatic forces, 2 fs for short-range non-bonded forces, and 1 fs for bonded forces. All bond lengths involving hydrogen atoms were held fixed using the SHAKE algorithm. A Langevin dynamics scheme was used for thermostating. Nose-Hoover-Langevin pistons were used for pressure control (9, 10). Molecular graphics and simulation analyses were generated with the VMD 1.8.3 software package (11). The simulation was carried out for 34 ns, but the analysis was performed over only the last 16 ns.

Supplementary Figures

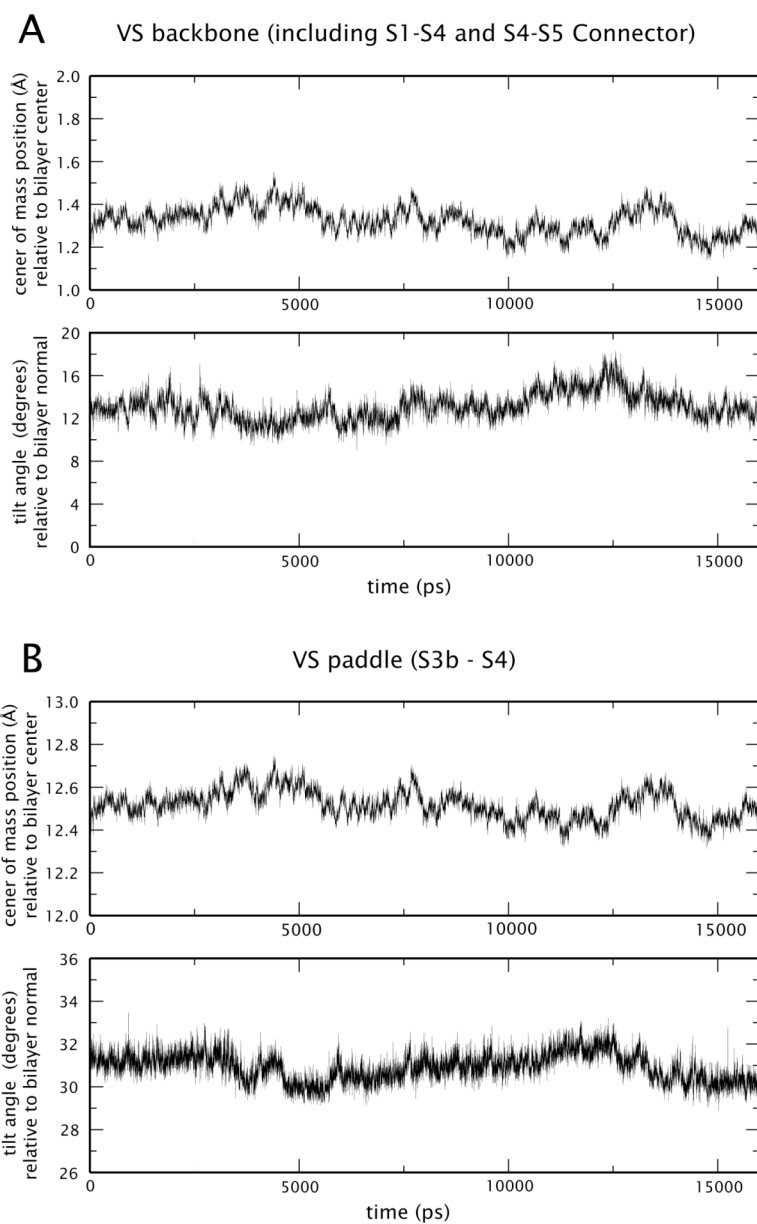


Figure S1. Trajectories of the center-of-mass and tilt-angle of (A) the entire KvAP voltage-sensor domain and (B) the voltage-paddle domain during the last 16 ns of the 34 ns simulation.

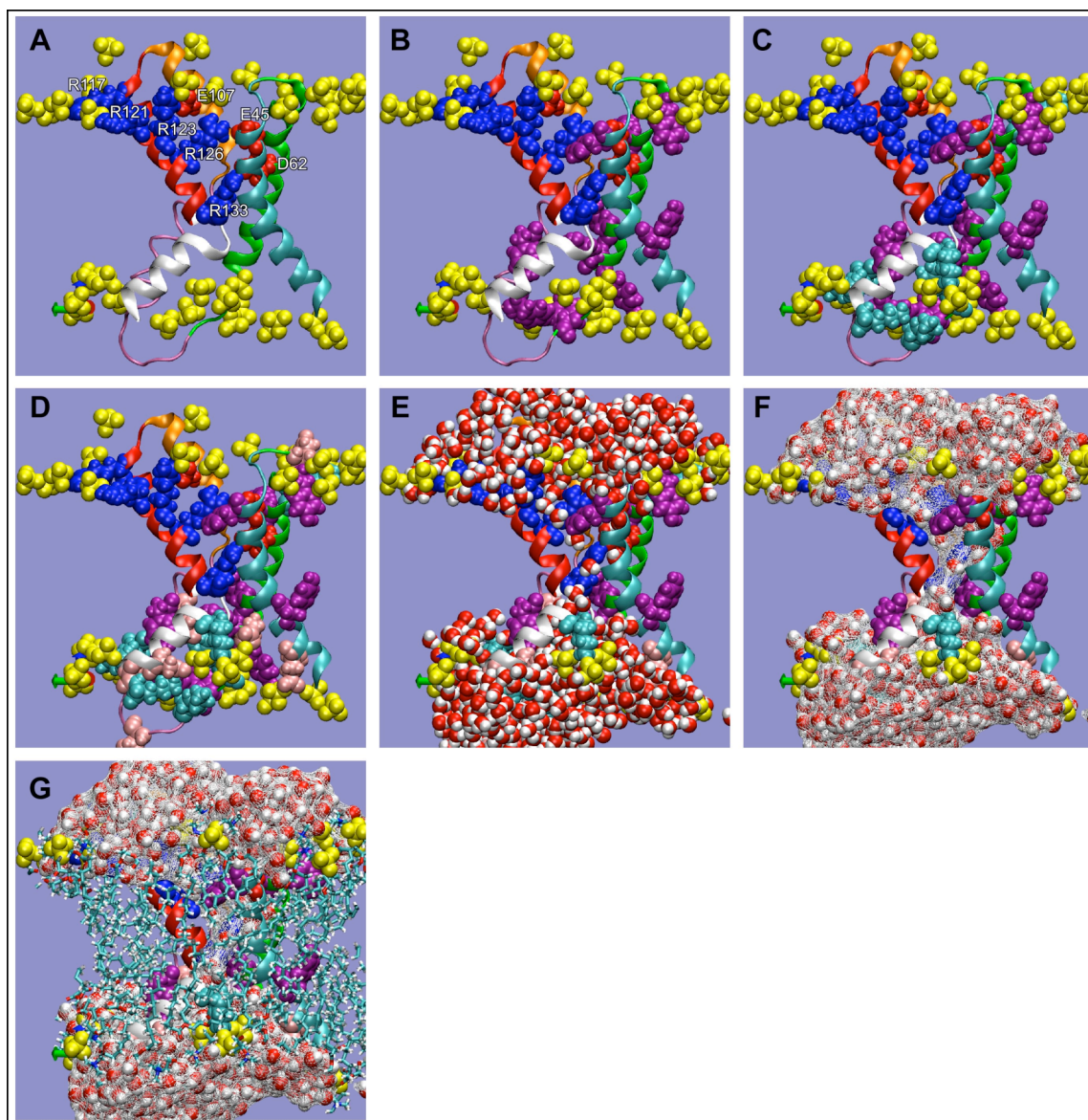


Figure S2. Building a voltage-sensor water pore. To clarify the organization of the water pore, a series of images shows the successive addition of key components. **(A)** Voltage sensor showing key arginine residues (blue spheres) and salt-bridge partners. Lipid phosphate groups (yellow spheres) form salt-bridge configurations with the sidechains of R117 and R121. One phosphate group appears in the first-coordination shell of R123. R123, R126, and R133 form salt-bridge configurations with acidic residues (red spheres) on the S3 and S2 helices (E107, E45, and D62, respectively). **(B)** Image A with Trp and Tyr residues (purple) added. Note that Trp residues in S3a remain at the lipid headgroup interface. **(C)** Image B with the rest of the VS basic residues (cyan) added. Note that lipid phosphate groups form salt-bridge configurations with some of these residues. **(D)** Image C with the remaining VS acidic residues (pink) added. Some of these residue form salt-bridges with basic residues. These interactions depicted in (A) to (D), orient the VS helices in the lipid bilayer to create the water-filled vestibules or crevices that penetrate to the membrane mid-plane from both membrane surfaces. **(E)** Image D with waters within 5 Å of the sensor added. Water molecules appear to coordinate all the polar residues located at the phospholipid headgroup interfaces. Some water molecules form

hydration sites for the buried salt-bridges. (F) Image E with a Connely surface (12) that highlights the continuity of the water H-bonding through the central salt-bridge R133-D62. (G) Image F with POPC lipids within 8 Å of the sensor added. Note that the acyl chains form an insulating cage around the sensor. A similar architecture has been reported for VS domains in a simulation of a model Kv1.2 potassium channel (13) and in a simulation of the KvAP VS in a detergent micelle (14). The overall configuration is in agreement with the water and lipid accessibility analysis reported by Cuello et al. (15) from EPR spectroscopy measurements on spin labeled mutants of the isolated VS of KvAP.

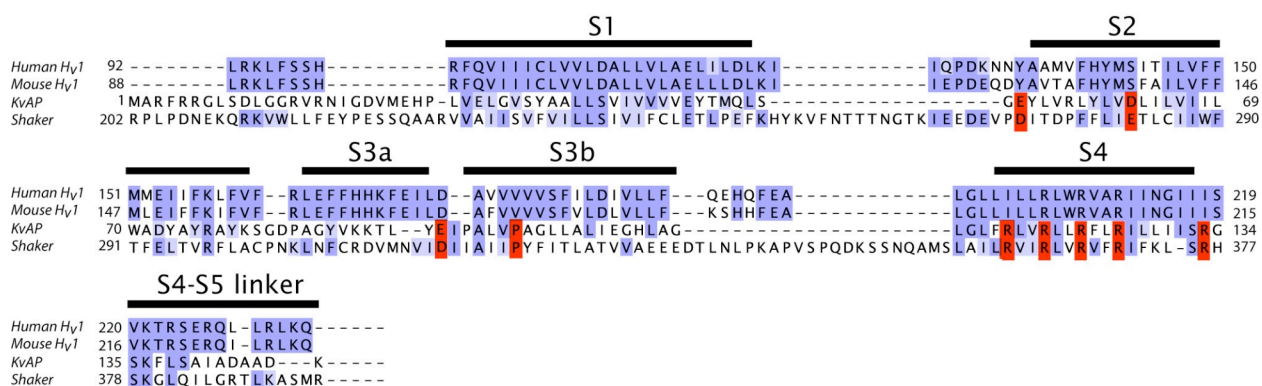


Figure S3. Alignment of the human and mouse *Hv1* sequences with the KvAP and Shaker voltage-sensor sequences. The alignment is an amalgam of the alignments by Ramsey et al. (16) and Jiang et al. (17).

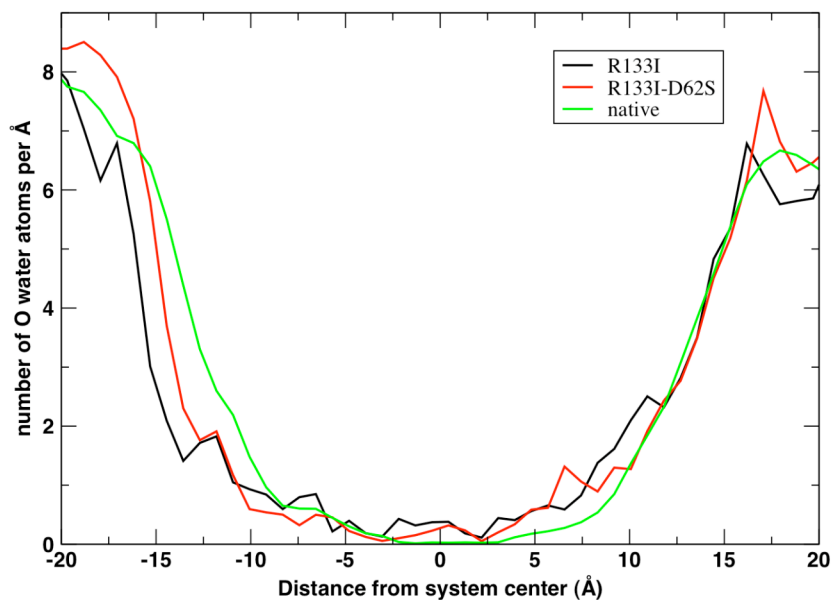


Figure S4. Water distribution along the transmembrane direction measured as density of water-water hydrogen-bond-like configurations. The curves for R133I and the native KvAP VS are the same as those presented in figures 2D and 2B.

References

1. Lee, S.-Y., A. Lee, J. Chen, and R. MacKinnon. 2005. Structure of the KvAP voltage-dependent K⁺ channel and its dependence on the lipid membrane. *Proc. Natl. Acad. Sci. USA* 102:15441-15446.
2. Kalé, L., R. Skeel, M. Bhandarkar, R. Brunner, A. Gursoy, N. Krawetz, J. Phillips, A. Shinozaki, K. Varadarajan, and K. Schulten. 1999. NAMD2: Greater scalability for parallel molecular dynamics. *J. Comput. Phys.* 151:283-312.
3. MacKerell, A. D., Jr., D. Bashford, M. Bellott, R. L. Dunbrack, Jr., J. D. Evanseck, M. J. Field, S. Fischer, J. Gao, H. Guo, S. Ha, D. Joseph-McCarthy, L. Kuchnir, K. Kuczera, F. T. K. Lau, C. Mattos, S. Michnick, T. Ngo, D. T. Nguyen, B. Prodhom, W. E. Reiher, III, B. Roux, M. Schlenkrich, J. C. Smith, R. Stote, J. Straub, M. Watanabe, J. Wiórkiewicz-Kuczera, D. Yin, and M. Karplus. 1998. All-atom empirical potential for molecular modeling and dynamics studies of proteins. *J. Phys. Chem. B* 102:3586-3616.
4. Feller, S. E., and A. D. MacKerell, Jr. 2000. An improved empirical potential energy function for molecular simulations of phospholipids. *J. Phys. Chem. B* 104:7510-7515.
5. Jorgensen, W. L., J. Chandrasekhar, J. D. Madura, R. W. Impey, and M. L. Klein. 1983. Comparison of simple potential functions for simulating liquid water. *J. Chem. Phys.* 79:926-935.
6. Darden, T., D. York, and L. Pedersen. 1993. Particle mesh Ewald: An $N \cdot \log(N)$ method for Ewald sums in large systems. *J. Chem. Phys.* 98:10089-10092.
7. Essmann, U., L. Perera, M. L. Berkowitz, T. Darden, H. Lee, and L. G. Pedersen. 1995. A smooth particle mesh Ewald method. *J. Chem. Phys.* 103:8577-8593.
8. Tuckerman, M., and B. J. Berne. 1992. Reversible multiple time scale molecular dynamics. *J. Chem. Phys.* 97:1990-2001.
9. Martyna, G. J., D. J. Tobias, and M. L. Klein. 1994. Constant-pressure molecular-dynamics algorithms. *J. Chem. Phys.* 101:4177-4189.
10. Feller, S. E., Y. Zhang, R. W. Pastor, and B. R. Brooks. 1995. Constant pressure molecular dynamics simulation: The Langevin piston method. *J. Chem. Phys.* 103:4613-4621.
11. Humphrey, W., W. Dalke, and K. Schulten. 1996. VMD: Visual molecular dynamics. *J. Mol. Graph.* 14:33-38.
12. Sanner, M. F., J.-C. Spohner, and A. J. Olson. 1996. Reduced surface: An efficient way to compute molecular surfaces. *Biopolymers* 38:305-320.
13. Treptow, W., and M. Tarek. 2006. Environment of the gating charges in the Kv1.2 *Shaker* potassium channel. *Biophys. J.* 90:L64-L66.
14. Sands, Z. A., A. Grottesi, and M. S. P. Sansom. 2006. The intrinsic flexibility of the Kv voltage sensor and its implications for channel gating. *Biophys. J.* 90:1598-1606.

15. Cuello, L. G., D. M. Cortes, and E. Perozo. 2004. Molecular architecture of the Kvap voltage-dependent K⁺ channel in a lipid bilayer. *Science* 306:491-495.
16. Ramsey, I. S., M. M. Moran, J. A. Chong, and D. E. Clapham. 2006. A voltage-gated proton-selective channel lacking the pore domain. *Nature* 440:1213-1216.
17. Jiang, Y. X., A. Lee, J. Y. Chen, V. Ruta, M. Cadene, B. T. Chait, and R. MacKinnon. 2003. X-ray structure of a voltage-dependent K⁺ channel. *Nature* 423:33-41.